

## ARTICLES

## Tuning the Vibrational Relaxation of CO Bound to Heme and Metalloporphyrin Complexes

Jeffrey R. Hill, Christopher J. Ziegler, Kenneth S. Suslick, and Dana D. Klott\*

*School of Chemical Sciences, University of Illinois at Urbana–Champaign, 505 S. Mathews Avenue, Urbana, Illinois 61801*

C. W. Rella

*Hansen Experimental Physics Laboratory, Stanford University, Stanford, California 94305*

M. D. Fayer\*

*Department of Chemistry, Stanford University, Stanford, California 94305**Received: May 16, 1996; In Final Form: August 7, 1996*<sup>⊗</sup>

Picosecond mid-infrared pump–probe experiments were used to investigate vibrational relaxation (VR, which here denotes loss of excess vibrational energy) of CO bound to synthetic heme and porphyrin complexes with different metal atoms (M = Fe, Ru, Os) and different proximal ligands (imidazoles and pyridines). Isotope effects of <sup>13</sup>CO vs <sup>12</sup>CO and solvent effects were also studied. A remarkable correlation between the carbonyl vibrational lifetime and the carbonyl vibrational frequency  $\nu_{\text{CO}}$  is observed. The vibrational lifetime decreases as  $\nu_{\text{CO}}$  decreases. The lifetime–frequency correlation is consistent with a linear relation between carbonyl vibrational relaxation rate and  $\nu_{\text{CO}}$ . Hemes and porphyrins show similar lifetime–frequency correlations, but the absolute value of the VR rate in *meso*-tetraphenylporphyrin complexes is slightly faster than in protoporphyrin IX dimethyl ester heme complexes. The predominant VR process is shown to be intramolecular transfer from CO to heme vibrations, rather than intermolecular transfer from CO to solvent vibrations. The intramolecular process occurs by anharmonic coupling via  $\pi$ -bonding between CO and the metalloporphyrin or heme. In metalloporphyrin and heme complexes, changes in back-bonding to CO simultaneously affect both CO frequency and the strength of anharmonic coupling, accounting for the observed lifetime–frequency correlation. Increasing back-bonding lowers the CO frequency and increases the anharmonic coupling, shortening the vibrational lifetime. Similar lifetime–frequency correlations are observed in wild-type and mutant heme proteins. It is possible to continuously tune the vibrational relaxation rate of CO over a range spanning about a factor of 4, by systematic modification of the chemical structure of the heme or porphyrin complex to which it is bound.

## I. Introduction

In order to better understand the relationships between molecular structure and vibrational dynamics, we have investigated the rates of vibrational relaxation (VR) of carbon monoxide (CO) bound to the active site of synthetic heme and porphyrin complexes. A brief communication of some of this work appeared recently.<sup>1</sup> Here VR is used to denote *vibrational energy relaxation*, the loss of energy from vibrationally excited CO to the rest of the system. VR rates were determined using picosecond mid-infrared (mid-IR) pump–probe experiments. We focus our attention on heme and metalloporphyrin complexes, because well-developed techniques of synthetic chemistry and genetic engineering permit systematic control over the structure, both in these synthetic analogs of heme proteins and in heme proteins themselves. In addition, these studies are expected to provide additional insight into how heme protein structure influences molecular dynamics at the active site of a protein.<sup>2–6</sup>

Loss of vibrational energy from CO involves anharmonic coupling<sup>7</sup> between the carbonyl vibrational fundamental and its

surroundings. In broad terms, there are three ways this might occur,<sup>4</sup> as illustrated schematically in Figure 1. VR might be a purely intramolecular process, involving energy transfer from the CO vibration to heme or porphyrin vibrations, via the metalloporphyrin–CO bonds. We will call this process CO-to-porphyrin transfer. There are both  $\sigma$ - and  $\pi$ -orbitals involved in metalloporphyrin–CO bonding; the  $\pi$ -bonds are formed by back-bonding, i.e., back-donation from the metalloporphyrin  $d_{\pi}$  and  $p_{\pi}$  orbitals to the  $\pi^*$ -antibonding orbitals of CO.<sup>8</sup> Alternatively, carbonyl VR might be a purely intermolecular process, involving energy transfer from the CO vibration to solvent vibrations, via nonbonded interactions. We will call this process CO-to-solvent transfer. The CO-to-porphyrin or CO-to-solvent processes might also involve excitations of the low-frequency collective vibrations of the solvent (instantaneous normal modes or solvent phonons<sup>9</sup>). These processes may be distinguished by systematically varying the porphyrin structure, the solvent, the temperature, etc. The series of complexes studied here are variations on the canonical heme protein structure found in myoglobin, hemoglobin, and peroxidase, where the porphyrin is iron(II) protoporphyrinate IX (protoheme), the proximal axial ligand is the imidazole group of the amino acid histidine, and

<sup>⊗</sup> Abstract published in *Advance ACS Abstracts*, November 1, 1996.

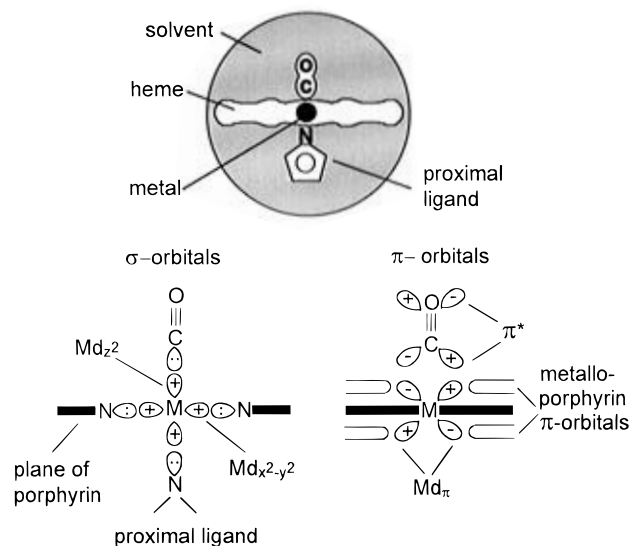


**Figure 1.** Schematic diagram of CO bound to a heme or porphyrin complex in a solvent. M denotes a metal atom. Loss of vibrational energy from CO excited by a mid-IR picosecond laser pulse might involve intramolecular CO-to-porphyrin vibration processes, intermolecular CO-to-solvent vibration processes, or a mixed process involving intra- or intermolecular vibrations and solvent phonons. CO-to-porphyrin processes must depend on metal-to-CO bonding. M–CO bonding involves both  $\sigma$ - and  $\pi$ -orbitals. The M–CO  $\pi$ -bonds are formed by back-donation of electrons from the metalloporphyrin macrocycle to antibonding  $\pi^*$  orbitals of CO.

the “solvent” is the surrounding protein.<sup>10</sup> We varied the structure of the complex using different metal atoms M in an isoelectronic series (M = Fe, Ru, Os), different porphyrins (which are the ligands *cis* to the CO), and different proximal (*trans*) ligands. In addition, experiments were performed using different solvents and isotopic substitution with <sup>13</sup>CO.

In previous work, mid-IR pump–probe experiments were used to investigate VR of CO bound to wild-type myoglobin (Mb),<sup>2–6</sup> mutant myoglobins,<sup>3</sup> and a heme complex containing either Fe, Ru, or Os.<sup>1,11</sup> These experiments suggested the possibility of a correlation between  $\nu_{\text{CO}}$ , the fundamental frequency of the carbonyl stretching transition, and the VR lifetime. The observed trends were rationalized by proposing the dominant mechanism of VR to involve intramolecular anharmonic coupling from CO to heme, via the heme–CO  $\pi$ -bonds, rather than the heme–CO  $\sigma$ -bonds. We argued that the dominant mechanism was “through  $\pi$ -bond coupling” rather than “through  $\sigma$ -bond coupling”.<sup>1,11</sup> Structural factors that increase back-bonding decrease both  $\nu_{\text{CO}}$  and the VR lifetime by increasing the through  $\pi$ -bond coupling.<sup>1–3,11</sup> In the prior study, only three variants of a single heme complex<sup>11</sup> were studied, so our proposed correlation was speculative but not definitive. In this work, we have investigated a large number of heme and porphyrin complexes, and we find a *remarkable* correlation between the vibrational lifetime and the carbonyl stretching frequency.<sup>1</sup> By modifying the complex structure, through changing the heme or porphyrin, the metal atom, or the proximal axial ligand, it becomes possible to tune the vibrational relaxation lifetime of CO over about a factor of 4. Never before has virtually continuous control of a vibrational lifetime been observed in a condensed phase polyatomic molecule.<sup>1</sup>

## II. Experimental Section

The preparation of the heme and porphyrin compounds used here followed standard literature methods, similar to those for preparing the coproporphyrinate I compounds described in more

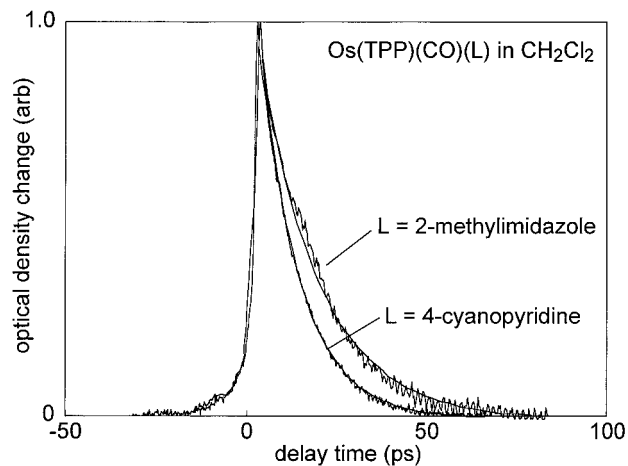


**Figure 2.** Some representative pump–probe data obtained on a porphyrin complex, Os(TPP)(CO)(L) in  $\text{CH}_2\text{Cl}_2$  solvent. TPP denotes 5,10,15,20-tetraphenylporphyrin. The smooth curves through the data are fits to single-exponential functions with time constants of 14.8 and 10.9 ps for proximal ligands L = 4-cyanopyridine and 2-methylimidazole. All the decay constants obtained in this work are given in Table 1.

detail in ref 11. For brevity, we will use the following abbreviations throughout: coproporphyrinate I tetraisopropyl ester = COPRO, 5,10,15,20-tetraphenylporphyrin = TPP, protoporphyrinate IX dimethyl ester = PHDME, and protoporphyrinate IX = PPIX. Fe porphyrins and free-base porphyrins were purchased from Aldrich Chemical. Fe(PHDME)(Cl) and Fe(TPP)(Cl) were dissolved in  $\text{CH}_2\text{Cl}_2$ , and a 2-fold excess of the appropriate proximal ligand was added. The Fe was reduced with sodium dithionite, and CO was added. The Ru and Os porphyrin carbonyls were synthesized from free-base porphyrins using  $\text{Ru}_3(\text{CO})_{12}$  and  $\text{Os}_3(\text{CO})_{12}$ .<sup>12,13</sup> Crystals of the Ru and Os porphyrin carbonyls are stable in air. These crystals could be dissolved in various solvents containing an excess of the desired proximal ligand. Fourier transform IR (FTIR) spectra were measured to verify purity and to determine  $\nu_{\text{CO}}$ . All the compounds used here had a single dominant conformer, as evidenced by the appearance of a single carbonyl stretching transition (e.g., see Figure 6a). The <sup>13</sup>CO forms of Ru(COPRO) and Os(COPRO) were synthesized from the <sup>12</sup>CO compounds, by irradiating solutions of the <sup>12</sup>CO carbonyls under an atmosphere of <sup>13</sup>CO with visible light. FTIR was used to verify that the exchange of <sup>13</sup>CO for <sup>12</sup>CO was complete (cf. Figure 6a).

Pump–probe measurements were performed at the Stanford Free Electron Laser Center. Details of the free electron laser (FEL), the experimental apparatus, and an explanation of pump–probe experiments are presented in ref 4. The pump–probe experiment measures the vibrational lifetime of the CO stretching mode,<sup>1,2,14–17</sup> which for the compounds studied here lies in the 1880–1980  $\text{cm}^{-1}$  range (5.05–5.38  $\mu\text{m}$ ).

## III. Results

All the pump–probe decay data obtained in this study were well fit by a single-exponential function of the form  $S(t) = S_0 \exp(-t/T_1)$ , where  $T_1$  is the lifetime of vibrationally excited ( $\nu = 1$ ) CO bound to porphyrin. For example, Figure 2 shows some representative pump–probe data obtained on a porphyrin, Os(TPP)(CO)(L) in  $\text{CH}_2\text{Cl}_2$  solvent, with two different proximal ligands (L). Table 1 lists all the vibrational lifetimes measured in this work. The error bounds on the values of  $T_1$  are estimated at  $\pm(1-2)$  ps. Also given in the table are the carbonyl stretching frequencies. The errors in frequency, estimated at  $\pm 1 \text{ cm}^{-1}$ ,

**TABLE 1: Vibrational Lifetimes and Vibrational Frequencies of CO Bound to Porphyrin Compounds. The Solvent Is CH<sub>2</sub>Cl<sub>2</sub> unless Otherwise Noted**

	tetraphenyl porphyrin (TPP)		protoporphyrin IX dimethyl ester (PHDME)	
	carbonyl freq (cm <sup>-1</sup> )	vib relaxation lifetime T <sub>1</sub> (ps)	carbonyl freq (cm <sup>-1</sup> )	vib relaxation lifetime T <sub>1</sub> (ps)
Fe Compounds				
pyridine	1975	32.5	1968	43.3
4-aminopyridine	1969	35.6	1963	44.5
Ru Compounds				
pyridine	1943	15.6	1934	17.3
4-aminopyridine	1938	16.6	1930	12.3
4-cyanopyridine	1948	18.3	1943	18.5
imidazole	1936	16	1927	15.5
2-methylimidazole	1936	15	1927	19.2
triphenylphosphine	1958	16.5	1946	13
Os Compounds				
pyridine	1912	12.6	1898	10.6
4-aminopyridine	1903	12.2	1891	12
4-cyanopyridine	1918	14.8	1903	12.9
imidazole	1899	11.1	1887	11.6
2-methylimidazole	1897	10.9	1887	11.6
triphenylphosphine	1928	10.7	1893	12.4
Solvent Effect on Ru(TPP)(CO)(pyridine)				
CH <sub>2</sub> Cl <sub>2</sub>	1943	15.6		
CHCl <sub>3</sub>	1937	15.8		
CCl <sub>4</sub>	1948	19		
CH <sub>3</sub> CCl <sub>3</sub>	1949	16.1		
dibutyl phthalate (DBP)	1949	11.5		
Isotope Effects				
Ru(COPRO) (pyridine)( <sup>13</sup> CO)	1880	19.5		
Os(COPRO) (pyridine)( <sup>13</sup> CO)	1860	12.9		

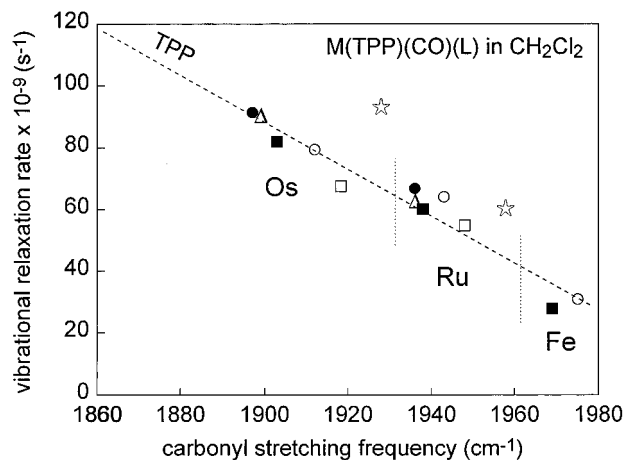


**Figure 3.** Carbonyl vibrational relaxation (VR) rate versus carbonyl stretching frequency  $\nu_{\text{CO}}$  for a series of tetraphenylporphyrin complexes  $M(\text{TPP})(\text{CO})(\text{L})$  in  $\text{CH}_2\text{Cl}_2$  solvent. The metal atom  $M$  is Fe, Ru, or Os as indicated. The proximal ligands  $L$  = pyridine ( $\circ$ ), imidazole ( $\Delta$ ), 2-methylimidazole ( $\bullet$ ), 4-aminopyridine ( $\blacksquare$ ), 4-cyanopyridine ( $\square$ ), and triphenylphosphine ( $\star$ ). The dashed line is a least-squares fit, neglecting the triphenylphosphine data.

are not instrument-limited. Instead, they arise from uncertainties in determining the peak frequencies of transitions with spectral widths in the 10–20  $\text{cm}^{-1}$  range.

**a. TPP and PHDME.** In Figure 3, we plot the VR rate versus carbonyl stretching frequency for TPP complexes. These data refer to  $M(\text{TPP})(\text{CO})(\text{L})$  in  $\text{CH}_2\text{Cl}_2$  solution. We used three different metal atoms ( $M = \text{Fe}, \text{Ru}, \text{Os}$ ) and six proximal ligands. A total of 14 different compounds were studied. The data on these compounds in Figure 3 show a high degree of correlation between the VR rate and the carbonyl stretching frequency  $\nu_{\text{CO}}$ . The VR rate *increases* as  $\nu_{\text{CO}}$  *decreases*. This relationship will be referred to as a lifetime–frequency correlation. The lifetime (inverse of the VR rate constant)

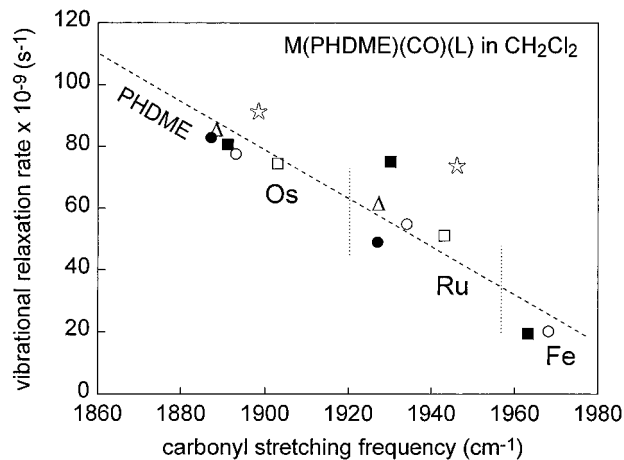


**Figure 4.** Carbonyl vibrational relaxation (VR) rate versus carbonyl stretching frequency  $\nu_{\text{CO}}$  for a series of protoheme dimethyl ester compounds  $M(\text{PHDME})(\text{CO})(\text{L})$  in  $\text{CH}_2\text{Cl}_2$  solvent. The proximal ligands  $L$  = pyridine ( $\circ$ ), imidazole ( $\Delta$ ), 2-methylimidazole ( $\bullet$ ), 4-aminopyridine ( $\blacksquare$ ), 4-cyanopyridine ( $\square$ ), and triphenylphosphine ( $\star$ ). The dashed line is a least-squares fit, neglecting the triphenylphosphine data.

*decreases* as  $\nu_{\text{CO}}$  *decreases*. As discussed later, the two complexes with triphenylphosphine ( $(\text{C}_6\text{H}_5)_3\text{P}$ ) as the axial ligands, denoted by stars in Figure 3, are exceptions to the observed correlation. Neglecting these two data points, the data in Figure 3 are well fit by a linear relationship, at least over this frequency range. The dashed line in Figure 3 is obtained using linear least-squares fitting, excluding the triphenylphosphine data.

Figure 4 shows the PHDME data. These data refer to  $M(\text{PHDME})(\text{CO})(\text{L})$  complexes in  $\text{CH}_2\text{Cl}_2$  solution. A strong correlation between VR rate and  $\nu_{\text{CO}}$  is again observed with the exception of the compounds with triphenylphosphine

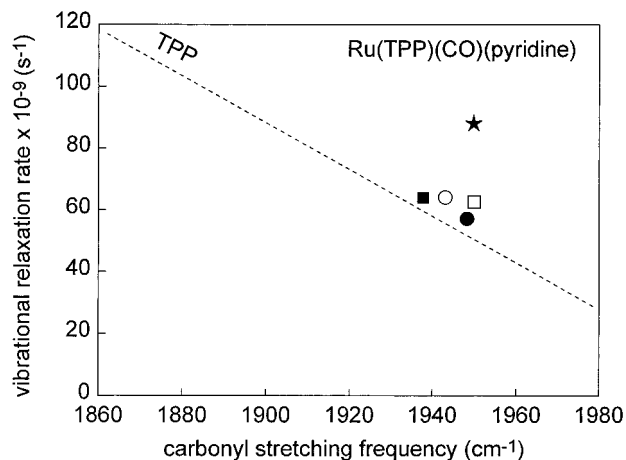


**Figure 5.** Solvent effects on the carbonyl vibrational relaxation (VR) rate of Ru(TPP)(CO)(pyridine). The solvents were CCl<sub>4</sub> (●), CHCl<sub>3</sub> (■), CH<sub>2</sub>Cl<sub>2</sub> (○), CH<sub>3</sub>CCl<sub>3</sub> (□), and dibutylphthalate (★). The dashed line is fit to the TPP data in Figure 3.

proximal ligands. Neglecting the triphenylphosphine data, linear least-squares fitting was used to determine the dashed line in Figure 4.

In both TPP and PHDME, the vibrational lifetimes are quite sensitive to the value of  $\nu_{\text{CO}}$ . Over a range ( $\sim 1900$ – $1980$  cm<sup>-1</sup>) where  $\nu_{\text{CO}}$  changes by  $\sim 4\%$ , the CO vibrational lifetimes range over a factor of  $\sim 4$  (the longest lifetimes are  $\sim 45$  ps and the shortest  $\sim 11$  ps).

In comparing the TPP and PHDME data, the slopes of the best-fit lines through the data are identical to within experimental error; however, the intercepts are slightly different. In our analysis, this difference appears to be statistically significant. At a given frequency, the VR rates of TPP compounds are on average about 10% faster than the VR rates of PHDME compounds.

**b. Solvent Effects.** The effects of different solvents on Ru(TPP)(CO)(pyridine) were studied. The solvents were CCl<sub>4</sub>, CHCl<sub>3</sub>, CH<sub>2</sub>Cl<sub>2</sub>, CH<sub>3</sub>CCl<sub>3</sub>, and dibutyl phthalate (DBP). There are small CO frequency shifts in the different solvents. Relative to the 1943 cm<sup>-1</sup> value in CH<sub>2</sub>Cl<sub>2</sub> solvent, which was the solvent used in all the other experiments,  $\nu_{\text{CO}}$  is blue-shifted by 5–6 cm<sup>-1</sup> in CCl<sub>4</sub>, CH<sub>3</sub>CCl<sub>3</sub>, and DBP, and  $\nu_{\text{CO}}$  is red-shifted 6 cm<sup>-1</sup> in CHCl<sub>3</sub> (see Table 1). The VR lifetimes in three chlorinated hydrocarbons CHCl<sub>3</sub>, CH<sub>3</sub>CCl<sub>3</sub>, and CH<sub>2</sub>Cl<sub>2</sub> were almost identical (Figure 5),  $\sim 16$  ps. In CCl<sub>4</sub> the lifetime is slightly longer, 19 ps. The effects on VR of these four solvents are smaller than changing the porphyrin from TPP to PHDME. In contrast, DBP has a noticeable influence on the VR rate. In DBP, the VR lifetime of 11.5 ps is  $\sim 40\%$  shorter than in CH<sub>2</sub>Cl<sub>2</sub>. As shown in Figure 5, there is no apparent correlation between the relatively small solvent-induced frequency shifts and changes in the VR lifetimes.

**c. Isotope Effects.** The effects of substituting <sup>13</sup>CO for <sup>12</sup>CO are shown in Figures 6 and 7. We studied M(COPRO)(CO)(pyridine) in CH<sub>2</sub>Cl<sub>2</sub> solvent, where M = Ru, Os. Figure 6 shows data on the Ru compound. The mid-IR spectrum in Figure 6a shows that <sup>13</sup>CO produces a substantial frequency red shift. The pump–probe data in Figure 6b show the pump–probe decays of the <sup>12</sup>CO and <sup>13</sup>CO compounds are virtually indistinguishable, in spite of the substantial frequency shift. Figure 7 is a plot of the isotope effect data on Ru and Os compounds versus  $\nu_{\text{CO}}$ . Based on the dependence of VR rate on  $\nu_{\text{CO}}$  seen in Figures 3 and 4, the CO frequency reduction due to <sup>13</sup>CO would be expected to roughly double the VR rate. Figure 7 shows instead that the effect of <sup>13</sup>CO on VR rate is

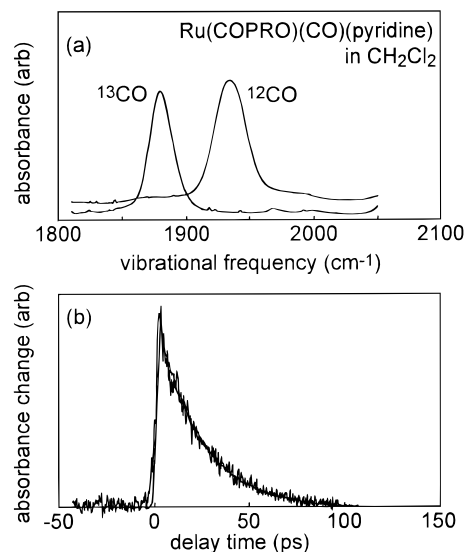


**Figure 6.** Isotope effect data on a coproporphyrin compound, M(COPRO)(CO)(pyridine). (a) Infrared spectra of <sup>12</sup>CO and <sup>13</sup>CO bound to Ru(COPRO)(pyridine), showing a sizable isotope frequency shift. (b) The pump–probe decays for both <sup>12</sup>CO and <sup>13</sup>CO species are shown. The decays are virtually indistinguishable, showing isotopic substitution has no appreciable effect on the VR rate.

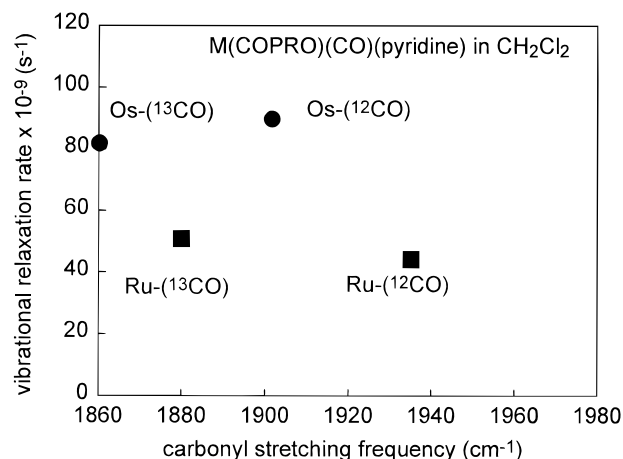


**Figure 7.** Plot of isotope effects on carbonyl VR using <sup>12</sup>CO and <sup>13</sup>CO forms of Ru(COPRO)(CO)(pyridine) and Os(COPRO)(CO)(pyridine) in CH<sub>2</sub>Cl<sub>2</sub> solution. Isotopic substitution induces a substantial frequency shift but has almost no effect on VR rate.

quite small, at most a few percent. In fact, any differences in VR rates between <sup>12</sup>CO and <sup>13</sup>CO compounds seen in Figure 7 are likely within the errors of our measurement. Therefore, there is essentially no isotope effect on the VR rate.

#### IV. The Vibrational Relaxation Process

A brief discussion of the VR process will prove useful in interpreting our results. In pump–probe experiments,<sup>4</sup> a picosecond duration mid-IR pulse is tuned to the fundamental vibrational transition of CO (the  $\nu = 0$  to  $\nu = 1$  transition, in the 1860–1980 cm<sup>-1</sup> range). The excitation produced by the pulse is essentially localized on CO. This CO oscillator may, to a good degree of accuracy, be treated as a two-level system because the mid-IR pulses are not resonant with the  $\nu = 1$  to  $\nu = 2$  transition. The frequency bandwidth of the pumping pulses is less than the vibrational anharmonicity<sup>5</sup> of  $\sim 25$  cm<sup>-1</sup>.

The excited CO oscillator loses its excess vibrational energy via anharmonic coupling with the surrounding medium. This coupling is weak<sup>7</sup> in the sense that the period of oscillation ( $\sim 20$  fs) is far less than the typical lifetime ( $\sim 20$  ps). The VR rate

depends on the density of states in the medium at the frequency  $\nu_{\text{CO}}$  and the strength of coupling to those states. The combined effects of these two quantities, state density and coupling strength, are conveniently combined in the concept of the force correlation function.<sup>7,18</sup>

The vibrational modes of the medium produce a broad spectrum of structural fluctuations that act on the system. In this case, the system is the CO oscillator. The force correlation function describes the magnitudes of all fluctuating forces exerted by the medium on the system.<sup>7,18</sup> The rate of vibrational energy loss from CO is proportional to the rate of transitions from  $\nu = 1$  to  $\nu = 0$ . This rate is proportional to the Fourier component of the force correlation function at  $\nu_{\text{CO}}$ .

In the classical mechanical treatment of the force correlation function,<sup>18</sup> the medium induces transitions only when the medium's vibrations are excited, for example when the medium is at finite temperature. Recently, a fully quantum mechanical treatment of the force correlation function was developed.<sup>7</sup> The quantum mechanical treatment shows it is not necessary for the medium's vibrations to be thermally populated for VR to occur. In the quantum mechanical treatment, the nonradiative relaxation of the carbonyl oscillator two-level system is seen to be analogous to the more familiar problem of a radiative transition driven by a radiation field. VR in the absence of thermal population of the medium's vibrations is analogous to spontaneous emission, where radiative relaxation occurs even in the absence of a radiation field. The rates of spontaneous VR processes are independent of temperature and are nonzero even at zero temperature. VR induced by thermally excited vibrations of the medium is analogous to stimulated emission in a radiative system. The rates of the VR stimulated emission processes increase with increasing temperature. The quantum mechanical treatment is important because temperature-dependent studies of VR in heme proteins<sup>2</sup> have shown the quantum mechanical process analogous to spontaneous emission dominates, even at ambient temperature.

The VR rate of CO reflects the fluctuating forces exerted by the medium on CO at a high frequency of  $\sim 2000 \text{ cm}^{-1}$ . These high-frequency motions are predominantly associated with higher frequency intramolecular vibrational modes of the medium, as opposed to lower frequency structural or conformational transitions.<sup>4</sup> CO is an unusual ligand in that its fundamental vibration falls into a frequency range where there are no other fundamental vibrations of either porphyrin or solvent. Vibrational energy transfer from CO to either porphyrin or solvent thus involves states which are combinations or overtones of fundamental vibrations or states which are combinations of vibrations and solvent phonons. The solvent phonons are a continuum of lower frequency collective states,<sup>9</sup> which range from zero frequency to a cutoff in the few hundreds of  $\text{cm}^{-1}$  range.

In polyatomic molecules, the density of vibrational states, consisting of fundamentals, overtones, and combinations, increases with increasing energy. At lower energies, the state density is discrete or sparse. At higher energies, the state density becomes large and essentially continuous. The frequencies where these sparse and dense regions occur depend on the size of the molecule. A large molecule such as porphyrin will have very many vibrational states at frequency  $\nu_{\text{CO}}$ ,<sup>19</sup> so there are a large number of possible energy-conserving pathways for carbonyl VR, involving CO-to-porphyrin vibrations. Vibrational energy transfer to molecules with continuous state densities do not require phonons. Transfer processes involving vibrations and simultaneous creation or annihilation of phonons are possible as well. These latter processes are termed phonon-

assisted VR processes. A small molecule such as  $\text{CHCl}_3$  has a sparse density of vibrational states at  $\nu_{\text{CO}}$ . Unless there is an unlikely coincidence, there will be no energy-conserving pathways for CO to  $\text{CHCl}_3$ . For vibrational energy transfer to molecules with sparse state densities, at least one solvent phonon from the phonon continuum is required to assure energy conservation.

VR is expected to be most efficient when the quantum number mismatch with the final state is minimal.<sup>7</sup> The states closest in energy to  $\nu_{\text{CO}}$  with the smallest quantum number mismatch are those consisting of two higher frequency vibrations in the  $\sim 1000 \text{ cm}^{-1}$  range, or two vibrations plus one phonon. For an extreme example, states consisting of 20  $\sim 100 \text{ cm}^{-1}$  phonons are unlikely to be well coupled to the CO oscillator due the poor quantum number mismatch.

## V. Discussion

**A. Summary of Relevant Experimental Results.** The most significant features of our results are (1) the striking correlation between VR lifetime and the carbonyl stretching frequency  $\nu_{\text{CO}}$ , as well as the precise degree to which the vibrational lifetime can be tuned by controlling heme structure, (2) the small but systematic porphyrin effect in which PHDME heme complexes generally have longer VR lifetimes than TPP porphyrin complexes, (3) the insensitivity of the VR rate to changes of solvent, and (4) the lack of an isotope effect ( $^{13}\text{CO}$  for  $^{12}\text{CO}$ ) on the vibrational lifetime, despite the substantial frequency shift induced by isotopic substitution. A small number of exceptions to the lifetime–frequency correlation and solvent insensitivity are also observed, as discussed below.

**B. Lifetime-Frequency Correlation.** Our data show that changes in  $\nu_{\text{CO}}$  are correlated with changes in the VR lifetime. The VR lifetime *decreases* as  $\nu_{\text{CO}}$  *decreases*. Other workers have previously correlated other quantities with  $\nu_{\text{CO}}$ . For example, correlations between  $\nu_{\text{CO}}$  and  $\nu_{\text{Fe-C}}$  were described by Li and Spiro,<sup>20</sup> who concluded that carbonyl frequency shifting was primarily controlled by changes in back-bonding. An increase in back-bonding simultaneously weakens the C–O bond and strengthens the Fe–C bond. Correlations between  $\nu_{\text{CO}}$  and  $^{13}\text{C}$  and  $^{17}\text{O}$  chemical shifts were reported by Guo et al.,<sup>21</sup> who concluded that changes both in carbonyl frequency and chemical shift parameters were caused by changes in the extent of back-bonding.<sup>21,22</sup>

As the carbonyl frequency changes, the change in the VR lifetime might be caused by either of two factors:<sup>7</sup> (1) a change in the number of available states or (2) a change in the anharmonic coupling between CO and the surrounding medium. The isotope effect experiments (as discussed in detail in section V.E.) clearly show that the vibrational lifetime changes are due to changes in the anharmonic coupling. Because changes in  $\nu_{\text{CO}}$  and the vibrational lifetime are affected by changing the structure of the porphyrin, it is strongly indicative that the coupling which is significant is the coupling between CO and porphyrin, rather than the coupling between CO and solvent. The solvent effect experiments (see section V.F.) confirm this to be the case for chlorinated hydrocarbon solvents. Thus, the lifetime–frequency correlation occurs because porphyrin structures that change  $\nu_{\text{CO}}$  similarly change the coupling between CO and porphyrin, and this coupling is the predominant factor that controls the rate of vibrational energy flow from CO to porphyrin.

**C.  $\sigma$ - and  $\pi$ -Bonds.** Since we see the VR lifetime to be well correlated with  $\nu_{\text{CO}}$ , a brief discussion of factors which affect  $\nu_{\text{CO}}$  is now presented. A vast literature exists concerning carbonyl vibrational frequencies and carbonyl bonding in

metal–carbonyl systems, which we will not attempt to summarize here. It is well-known that carbonyl stretching frequencies can be affected by *cis* or *trans* ligand effects.<sup>23</sup> In the heme complexes used here, *cis* refers to the tetradentate porphyrin ligand and *trans* to the monodentate proximal ligand.

Returning to Figure 1, we note that metal–CO bonding involves both  $\sigma$ - and  $\pi$ -bonds. *Cis* and *trans* ligands might affect either or both types of bonding. Changing  $\sigma$ - and  $\pi$ -bonding affects  $\nu_{\text{CO}}$  in different ways. Effects of changing  $\pi$ -bonding have been discussed extensively by many authors, e.g., refs 20–22 and 24–26, whereas effects of changing  $\sigma$ -bonding are ordinarily less significant and not discussed much. We need to consider  $\sigma$ -bonding here to interpret deviations from the lifetime–frequency correlation seen in our data.

A simple and useful way of understanding these effects is to consider an isolated linear triatomic molecule M–C–O.<sup>23,27</sup> In Herzberg's book,<sup>27</sup> analytical solutions are presented for the vibrational frequencies in terms of the atomic masses and bond force constants. To model the heme or porphyrin complexes, M should be considerably heavier than C or O, and the C–O force constant  $k_{\text{CO}}$  should be considerably larger than the M–C force constant  $k_{\text{MC}}$ . In this case, the  $\nu_3$  vibration (in Herzberg's notation) is primarily a C–O stretching vibration,<sup>27</sup> with a small amount of coupling with the M–C oscillator. In a harmonic oscillator, the frequency is proportional to  $(k/\mu)^{1/2}$ , where  $\mu$  is the reduced mass. Thus, it is approximately correct to view changes in  $\nu_{\text{CO}}$  as arising from changes in either  $k$  or  $\mu$ .

Structural or environmental factors which affect  $\pi$ -bonding change the extent of back-bonding from the metalporphyrin  $d_{\pi}$  and  $p_{\pi}$  orbitals to the antibonding  $\pi^*$  orbitals of CO.<sup>8</sup> Increased back-bonding decreases  $k_{\text{CO}}$ , which tends to decrease  $\nu_{\text{CO}}$ . Decreased back-bonding has the opposite effect.

Although the primary effect of changing back-bonding is to change the force constant  $k_{\text{CO}}$ , there is a secondary effect which may be viewed as a reduced mass effect. Increasing back-bonding, which reduces  $k_{\text{CO}}$ , simultaneously increases  $k_{\text{MC}}$ , and vice versa.<sup>20</sup> When  $k_{\text{MC}}$  increases, the reduced mass of the CO oscillator seems to increase, because a stronger M–C bond means CO oscillations involve increasing displacements of the heavier M atom. The reduced mass effect of changing  $\pi$ -bonding opposes the force constant effect. The net effect of increasing back-bonding is as follows: there is a decrease in  $\nu_{\text{CO}}$  due to the decrease in  $k_{\text{CO}}$ , but the decrease in  $\nu_{\text{CO}}$  is slightly offset by an increase due to increasing  $\mu$ . For example, using the equations in ref 27, it can be shown that reducing  $k_{\text{CO}}$  in FeCO to produce a 70  $\text{cm}^{-1}$  decrease in  $\nu_{\text{CO}}$  (e.g., from 1970 to 1900  $\text{cm}^{-1}$ ), the reduced mass effect offsets the decrease in  $\nu_{\text{CO}}$  by about 5  $\text{cm}^{-1}$ . The reduced mass effect is not discussed extensively in the literature, probably because it is a perturbation to the dominant force constant effect.

A similar reduced mass effect can result from changing the  $\sigma$ -bonding. Some ligands can affect the  $\sigma$ -bonding between M and C.<sup>23</sup> Increasing the strength of the M–C bond increases the reduced mass of the CO oscillator, decreasing  $\nu_{\text{CO}}$ . The important feature of  $\sigma$ -bonding needed for subsequent discussions is that changes in  $\sigma$ -bonding induced by different ligands can affect  $\nu_{\text{CO}}$  without significantly changing the back-bonding between M and CO.  $\sigma$ -bond effects induced by ligands thus provide a possible mechanism for changing  $\nu_{\text{CO}}$  without affecting through  $\pi$ -bond anharmonic coupling.

**D. Anharmonic Coupling through  $\sigma$ - and  $\pi$ -Bonds.** There have been extensive prior studies of M–CO bonding and the effects on  $\nu_{\text{CO}}$ .<sup>23</sup> The new and unique feature of the present study is the ability of picosecond infrared pump–probe experi-

ments to reveal vibrational relaxation processes which depend on *anharmonic coupling*. Prior to the development of infrared pump–probe techniques, essentially nothing was known about M–CO anharmonic coupling.

In a previous paper,<sup>11</sup> we argued that vibrational energy transfer from excited CO to heme principally involved through  $\pi$ -bond coupling, rather than through  $\sigma$ -bond coupling. The argument was based on three data points, corresponding to the heme compounds M(COPRO)(CO)(pyridine), where M = Fe, Ru, Os, in  $\text{CH}_2\text{Cl}_2$  solvent. It was known that  $\nu_{\text{CO}}$  decreases with increasing mass of the M atom. The heavier M atoms have more polarizable and more spatially extended valence electrons, which increase the extent of back-bonding.<sup>28,29</sup> Our finding was that the VR lifetime decreased as the mass of the M atom increased.<sup>11</sup>

The decrease in VR lifetime with increasing mass of the metal atom is exactly opposite what one expects if through  $\sigma$ -bond coupling were dominant.<sup>11,30</sup> From the viewpoint of classical mechanics, which presents a simple and intuitive picture of this process, the CO oscillator loses energy by driving the M–C oscillator. When the M atom is made heavier, the M–C oscillator is shifted further off-resonance from the CO oscillator, the amplitudes of M atom oscillations decrease, and the extent of through  $\sigma$ -bond coupling is decreased.<sup>6,11</sup> From the viewpoint of the mechanical force correlation function model in either the classical<sup>18</sup> or quantum pictures,<sup>7</sup> making the M atom heavier makes the modes associated with the heavier atom lower in frequency, resulting in smaller Fourier coefficients of the force correlation function at  $\nu_{\text{CO}}$ . In either description, heavier metal atoms must reduce through  $\sigma$ -bond coupling. Because heavier M atoms decreased the VR lifetime, the through  $\sigma$ -bond coupling mechanism can be convincingly ruled out.<sup>11</sup>

The evidence against through  $\sigma$ -bond coupling suggested that through  $\pi$ -bond coupling was dominant. More significantly, through  $\pi$ -bond coupling could be invoked to explain the direction of the observed relation between lifetime and frequency.<sup>11</sup> Increased back-bonding would be expected to decrease the VR lifetime by increasing through  $\pi$ -bond coupling, while lowering  $\nu_{\text{CO}}$ , as observed.<sup>11</sup> The lifetime–frequency correlations seen in Figures 3 and 4 thus provide compelling evidence for the dominance of through  $\pi$ -bond coupling in the relaxation of vibrationally excited CO bound to heme.

**E. Isotope Effects on Vibrational Relaxation.** The isotope effect experiments reveal a feature of the lifetime–frequency correlation which is crucial in understanding the mechanism of carbonyl VR. As shown in Figures 6 and 7, substituting <sup>13</sup>CO for <sup>12</sup>CO in heme compounds causes a substantial change of  $\nu_{\text{CO}}$  but no change in the VR lifetime. There is a negligible isotope effect on VR. A <sup>13</sup>CO experiment on Mb–CO gave the same result.<sup>3</sup> The isotope effect experiments clearly demonstrate the lifetime–frequency correlation does not depend on the absolute value of  $\nu_{\text{CO}}$ , but instead on the *induced shift* of  $\nu_{\text{CO}}$  caused by changing the chemical structure and thus the extent of back-bonding.

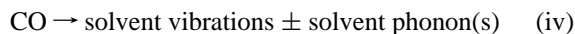
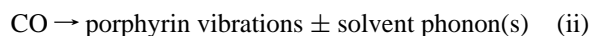
It is conceivable that the vibrational lifetime could depend on the absolute value of  $\nu_{\text{CO}}$  in such a way that decreasing  $\nu_{\text{CO}}$  decreased the lifetime. This situation could arise only if changes in the lifetime depended on changes in the density of states.<sup>3–4,7</sup> Such a dependence might exist, for instance, if the density of heme vibrational states at  $\nu_{\text{CO}}$  increased with decreasing  $\nu_{\text{CO}}$ . A similar dependence might be expected if there existed an energy mismatch between the carbonyl oscillator and some specific heme vibration or vibrations located at somewhat lower energy. Then decreasing  $\nu_{\text{CO}}$  would decrease the energy gap for this process, thereby decreasing the vibrational lifetime. In

either case,  $^{13}\text{CO}$  VR would have a significantly shorter lifetime than  $^{12}\text{CO}$  VR, which is not observed. The isotope experiments show that changes in the vibrational lifetime do not depend on the absolute value of  $\nu_{\text{CO}}$ , which rules out the possibility that the lifetime–frequency correlation is due to the structure of the density of heme states near  $\nu_{\text{CO}}$ . The lifetime–frequency correlation must therefore depend on changes in the anharmonic coupling between CO and heme or porphyrin, induced by changing the structure of the complex.

The lifetime–frequency correlation is thus understood as follows. Changing porphyrin substituents (e.g., the metal atom and proximal ligands) changes the extent of back-bonding. An increase in back-bonding lowers  $\nu_{\text{CO}}$ . An increase in back-bonding simultaneously increases through  $\pi$ -bond anharmonic coupling, which decreases the CO vibrational lifetime.

**F. Solvent Effects on Vibrational Relaxation.** The solvent effect experiments address the relative significance of intramolecular *vs* intermolecular VR processes in the lifetime–frequency correlation data in Figures 3 and 4, where  $\text{CH}_2\text{Cl}_2$  was the solvent. The observations which need to be discussed are the essentially identical ( $\sim 16$  ps) VR lifetimes of the Ru complex in  $\text{CH}_2\text{Cl}_2$ ,  $\text{CHCl}_3$ , and  $\text{CH}_3\text{CCl}_3$ , the slightly longer (19 *vs* 16 ps) VR lifetime in  $\text{CCl}_4$ , and the significant shortening ( $\sim 40\%$ ) of the VR lifetime in DBP.

To understand solvent effects, we must consider the four general mechanisms for loss of vibrational excitation from CO in a solvated porphyrin complex:



Unlikely processes such as  $\text{CO} \rightarrow$  (many solvent phonons) are not considered above. Processes i and iii involve energy transfer from the vibrationally excited CO to vibrational states of the porphyrin or the solvent. Processes ii and iv are phonon-assisted versions of processes i and iii. For any of these processes to occur, the solvent or porphyrin must have at least one state (i.e., a combination or overtone of vibrations and/or phonons) at frequency  $\nu_{\text{CO}}$ , and there must be anharmonic coupling between the CO stretching fundamental and the porphyrin or the solvent. It is straightforward to approximately determine the density of vibrational states of porphyrin or solvent using vibrational spectra or normal mode calculations, but the coupling is difficult to determine *a priori*, since anharmonic coupling depends on the finer details of the potential surface.<sup>7</sup>

In processes ii and iv, a plus sign indicates a phonon is emitted and a minus sign indicates a phonon is absorbed. Phonon absorption occurs only at finite temperature, where the phonons are thermally populated. Because phonon energies range from zero frequency to a frequency cutoff in the few hundred  $\text{cm}^{-1}$  range,<sup>9,32</sup> the phonon population changes greatly in the 0–300 K range (at 300 K,  $kT \sim 200 \text{ cm}^{-1}$ ). Temperature-dependent studies of VR<sup>2</sup> can be used to determine whether the dominant VR process is phonon-assisted. If phonons are involved, the rate of the VR process will change significantly in this temperature range.

Process i is a purely intramolecular CO-to-porphyrin transfer. The porphyrin density of states at  $\nu_{\text{CO}}$  is very large,<sup>19</sup> so process i can occur even without the solvent. Process i is the process which we believe dominates the VR of CO in porphyrin complexes and which is responsible for the lifetime–frequency correlation. For the solvent to affect the rate of process i, it

must affect the anharmonic coupling between CO and porphyrin. It is difficult to see how this proposed solvent effect mechanism could explain the data in Figure 5. The solvent effect on VR cannot simply be a change in the through  $\pi$ -bond anharmonic coupling between CO and porphyrin, because that would result in a lifetime–frequency correlation which is not observed. There are some solvents (e.g.,  $\text{CHCl}_3$  and  $\text{CH}_3\text{CCl}_3$ ) where  $\nu_{\text{CO}}$  differs somewhat (by  $12 \text{ cm}^{-1}$  in this case), but the VR rates are identical. In  $\text{CH}_3\text{CCl}_3$  and DBP,  $\nu_{\text{CO}}$  is identical, but the VR rates are quite different. For the solvent effect to occur by affecting the rate of process i, the solvent would somehow have to affect the anharmonic coupling in a new way which does not introduce a correlated frequency shift. We believe this to be unlikely.

Process ii is a solvent phonon-assisted transfer from CO to porphyrin. Changing the solvent changes both the solvent phonon densities of states and the strength of anharmonic coupling between the porphyrin complex and the solvent phonons. There are several reasons why we expect (but cannot yet prove positively) that this process is not significant in the porphyrin–CO complexes. First, phonons are not really necessary for the CO-to-porphyrin process, due to the large state density of porphyrin vibrations at  $\nu_{\text{CO}}$ . Second, the phonon densities of states of  $\text{CHCl}_3$  and  $\text{CH}_3\text{CCl}_3$  are different from that of  $\text{CH}_2\text{Cl}_2$ , but the VR lifetime is the same in all three of solvents. Third, we know from temperature-dependent studies<sup>2</sup> that this type of phonon-assisted CO-to-porphyrin process is not significant in Mb, which is quite similar to the porphyrin complexes we have studied.

Process iii is an intermolecular transfer from CO to solvent vibrations, without phonons. We will discuss DBP separately from the chlorinated hydrocarbons. These latter solvents are all rather small molecules, and they have a sparse density of vibrational states near  $\nu_{\text{CO}}$ . Using tabulated vibrational spectral data,<sup>31</sup> one can estimate the density of states near  $\nu_{\text{CO}}$  to decrease in the order  $\text{CH}_3\text{CCl}_3 > \text{CCl}_4 > \text{CHCl}_3 > \text{CH}_2\text{Cl}_2$ .  $\text{CH}_3\text{CCl}_3$  of course has the greatest density of vibrational states.  $\text{CCl}_4$  is next because it has four low-frequency C–Cl stretching vibrations. The latter two solvents have high-frequency C–H stretching vibrations which are too high in energy to interact with the CO oscillator. Due to the sparsity of solvent vibrational states at  $\nu_{\text{CO}}$ , it would be an unlikely coincidence if any solvent vibrational states were precisely resonant with the carbonyl oscillator. Thus, the likelihood of CO-to-solvent vibration transfer process iii (without phonons) is quite small in the chlorinated hydrocarbons. Furthermore, even if by a series of coincidences this process were possible *in all four of these solvents*, because the vibrational densities of states are very different, VR would be very different in each solvent, which is not observed.

Process iv is a phonon-assisted intermolecular transfer. Phonon assistance permits energy transfer from excited CO to solvent vibrations lying within a few hundred  $\text{cm}^{-1}$  of  $\nu_{\text{CO}}$ . Thus, process iv is the only way energy can be transferred from CO to a small solvent molecule which has a sparse vibrational density of states at  $\nu_{\text{CO}}$ . All other things remaining equal, the larger the value of the phonon cutoff frequency in a solvent, the more solvent vibrational states can participate in CO-to-solvent vibration transfer.

As above, energy transfer from CO to DBP can occur by process iv. However, the DBP solvent is a much larger molecule than the chlorinated hydrocarbon solvents. DBP molecules have a dense manifold of vibrational states at  $\nu_{\text{CO}}$ . Thus, energy transfer from vibrationally excited CO to DBP

vibrations can also occur by process iii, which is not possible in the chlorinated hydrocarbon solvents.

In light of the above discussion, we can offer some reasonable, but not definitive, interpretations of our solvent effect data. There is no evidence for *significant* CO-to-solvent processes (either processes iii or iv) in  $\text{CH}_2\text{Cl}_2$ , the solvent used to establish the lifetime–frequency correlation. Otherwise, the carbonyl VR rate would be significantly different in the different chlorinated hydrocarbon solvents, because their state densities at  $\nu_{\text{CO}}$  are very different. The slightly longer VR lifetime in  $\text{CCl}_4$  does suggest the possibility that a small fraction of the VR in  $\text{CH}_2\text{Cl}_2$  (as well as  $\text{CHCl}_3$  and  $\text{CH}_2\text{Cl}_2$ ) could be due to intermolecular vibrational energy transfer, most likely by process iv. A CO-to- $\text{CH}_2\text{Cl}_2$  process which was competitive with the CO-to-porphyrin process could account for the 19 to 16 ps lifetime reduction in going from  $\text{CCl}_4$  to  $\text{CH}_2\text{Cl}_2$ , if the CO-to- $\text{CH}_2\text{Cl}_2$  process had a lifetime of  $\sim 100$  ps at room temperature. If this relatively inefficient CO-to-solvent process does exist in  $\text{CH}_2\text{Cl}_2$ , there are two possibilities for explaining why it is absent (or is perhaps even more inefficient) in  $\text{CCl}_4$ . Either the relatively low-frequency solvent phonon cutoff in  $\text{CCl}_4$  reduces the number of energy-conserving pathways for CO-to-solvent transfer (notice here it would be the phonon spectrum of  $\text{CCl}_4$  which mattered, not the vibrational spectrum), or the nonpolar  $\text{CCl}_4$  interacts less strongly with the porphyrin–CO complex than other, more polar chlorinated hydrocarbon solvents.

The significant effect of DBP on the VR rate seems to be indicative of a CO-to-DBP transfer process. This intermolecular process may (iv) or may not (iii) involve phonons. The alternative to this interpretation is to postulate some mechanism for DBP to substantially change the CO-to-porphyrin anharmonic coupling without any effect on  $\nu_{\text{CO}}$ . The relative importance of phonons could be investigated by studying the temperature dependence of VR in DBP. The presumed ability of DBP to participate in intermolecular VR processes is a result of the large state density at  $\nu_{\text{CO}}$ , but it is also worth noting the possibility of relatively strong nonbonded interactions between the aromatic phenyl groups of DBP and porphyrin.

More work needs to be done to better understand questions raised by the solvent effect data. For example, it would be interesting to study a series of compounds in DBP to see whether a lifetime–frequency correlation exists in DBP solutions. It will also be interesting to expand the range of solvents used in this study and to perform temperature-dependent experiments to investigate the role of solvent–heme interactions in VR.

### G. Additional Features of Through $\pi$ -Bond Coupling.

The through  $\pi$ -bond model accounts for the most significant features of our data, namely, the existence of a lifetime–frequency correlation, and the direction of the correlation, i.e., lower frequency means shorter lifetime. However, without some embellishments, the simplest form of this model does not account for two features of our data: (1) Both PHDME heme complexes and TPP porphyrin complexes show lifetime–frequency correlations, but the absolute values of the lifetimes in PHDME and TPP are different (the lifetimes are somewhat longer in the heme). (2) All the imidazole and pyridine complexes in Figures 3 and 4 show a lifetime–frequency correlation, but the triphenylphosphine complexes deviate significantly from this correlation.

The fact there exists a small but discernible systematic difference in the lifetime–frequency correlation between TPP and PHDME is interesting. It shows that carbonyl VR rates do not depend entirely on the structure at the active site, but rather these rates can be influenced by substituents on the

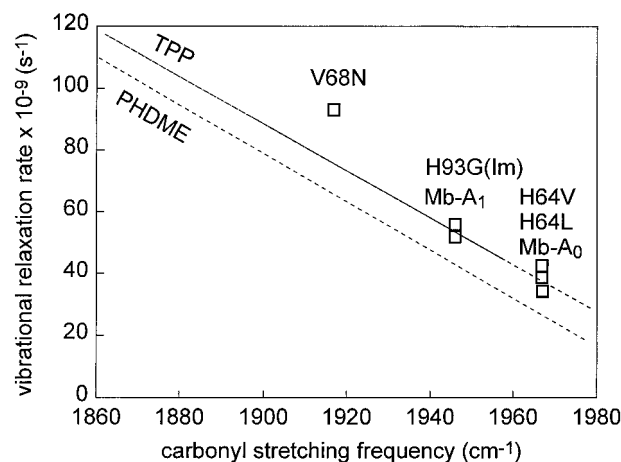


**Figure 8.** Comparison of synthetic heme compound data from this work to myoglobin–CO (Mb–CO) protein data from refs 2 and 3. The designations A<sub>0</sub> and A<sub>1</sub> refer to coexisting conformers of wild-type Mb–CO. H64L and H64V are mutants where the distal histidine is replaced by leucine or valine. H93G(Im) is a mutant where the proximal histidine is replaced by glycine, with added imidazole as the proximal ligand. V68N is a mutant where valine-68 is replaced by asparagine. The Mb data should be compared to Fe(PHDME), which is practically identical to protoheme in Mb. The Mb VR rates are clearly greater than in synthetic PHDME heme complexes. The greater VR rates in Mb are attributed to differences in solvent effects between PHDME in  $\text{CH}_2\text{Cl}_2$  compared to protoheme inside the protein matrix. The protein data also suggest a lifetime–frequency correlation similar to that seen in synthetic heme and porphyrin complexes in Figures 3 and 4.

porphyrin perimeter quite distant from CO. In previous works where correlations were found between  $\nu_{\text{CO}}$  and  $\nu_{\text{FeC}^{20}}$  or between  $\nu_{\text{CO}}$  and  $^{13}\text{C}$  coupling constants,<sup>21</sup> these correlations were said to apply equally well to heme proteins with PPIX and PHDME and TPP complexes. Systematic differences between these different porphyrin structures were not observed (or perhaps were not resolved). Besides resolving a clear difference between TPP and PHDME (Figures 3 and 4), as shown in the next section, we can also resolve clear differences between PHDME and heme proteins (cf. Figure 8).

The triphenylphosphine data in Figures 3 and 4 appear to be exceptions to the lifetime–frequency correlation. Something similar is seen in the frequency–chemical shift correlation data reported<sup>21</sup> by Guo et al. There the heme proteins P450 and chloroperoxidase<sup>21</sup> seem to be exceptions to their correlation. In our work and in their work, the systems which evidence these correlations all have proximal ligands which form metal–nitrogen bonds (histidine in the proteins, imidazoles, and pyridines in the synthetic heme complexes). The exceptions have quite different proximal bonding. There are metal–phosphorus bonds in the triphenylphosphine porphyrin complexes and metal–sulfur bonds in P450 and chloroperoxidase proteins, where histidine is replaced by cysteine. What appear to be exceptions to these correlations may not be exceptions at all. It is conceivable that a series of complexes with metal–phosphorus bonds or metal–sulfur bonds might themselves show a lifetime–frequency correlation. For example, the triphenylphosphine data are suggestive of a lifetime–frequency correlation for metal–phosphorus bonded systems which has only a slightly different slope and intercept from the correlation for metal–nitrogen bonded systems in Figures 3 and 4.

There are two orthogonal ways of looking at deviations from the lifetime–frequency correlation. For example, consider the triphenylphosphine data in Figure 3. If these data points are taken to lie *above* the line, then triphenylphosphine is causing the VR rate to increase without affecting  $\nu_{\text{CO}}$ . On the other



hand, if these data points are taken to lie to the *right* of the line, then triphenylphosphine is causing  $\nu_{\text{CO}}$  to increase without affecting the VR rate. These two possibilities require quite different interpretations, and either or both possibilities might be involved in causing the observed deviations. In the former case, triphenylphosphine is not affecting  $\nu_{\text{CO}}$ , but it is providing additional fluctuating forces on CO to increase the VR rate. The through  $\pi$ -bond coupling remains the same, but the three phenyl groups provide additional state density for the VR process. In the latter case, triphenylphosphine is causing a shift in  $\nu_{\text{CO}}$  without affecting the magnitude of the force correlation function at CO. This could occur, for instance, if triphenylphosphine shifted  $\nu_{\text{CO}}$  by changing the M–CO  $\sigma$ -bonding. As discussed in section V.C, ligands which affect the M–C  $\sigma$ -bonding can affect  $\nu_{\text{CO}}$  without affecting the  $\pi$ -bonding and the through  $\pi$ -bond anharmonic coupling.

In the same spirit, we now consider the PHDME vs TPP data (see the dashed lines in Figure 5). For a given value of  $\nu_{\text{CO}}$ , TPP compounds on average have faster VR rates. This might be interpreted to mean that the phenyl substituents on TPP compounds increase the fluctuating forces on CO to increase the VR rate without affecting  $\nu_{\text{CO}}$ . Alternatively, TPP could affect  $\nu_{\text{CO}}$ , perhaps by changing the M–CO  $\sigma$ -bonding, without significantly increasing the fluctuating forces on CO. Resolving these questions will require additional studies on more heme and porphyrin compounds or an independent probe of the extent of  $\sigma$ - and  $\pi$ -bonding in each compound.

**H. Proteins and Synthetic Hemes.** Our synthetic heme complexes provide new insights into pump–probe experiments on Mb–CO.<sup>2,3</sup> In Figure 8 we compare Mb VR data from refs 2 and 3 to the PHDME and TPP data from this work. Shown in Figure 8 are data<sup>2</sup> on two different conformers of wild-type horse heart Mb, denoted A<sub>0</sub> and A<sub>1</sub>. These conformers coexist in protein solutions. They are thought to arise from different states of the distal histidine.<sup>22</sup> Also shown are data<sup>3</sup> for several myoglobin mutants, including V68N, where valine-68 is replaced by asparagine. This substitution is interesting because it produces a particularly large shift<sup>25</sup> in  $\nu_{\text{CO}}$ , almost as large as substituting Os for Fe.

The data in Figure 8 suggest the existence of a lifetime–frequency correlation for proteins,<sup>3,4</sup> similar to the synthetic heme complexes. Because PPIX in Mb is only very slightly different from PHDME (in PHDME, two carboxylate groups on the perimeter of PPIX are esterified), the Mb data in Figure 8 should be compared to the PHDME data, rather than the TPP data. In comparing Mb to PHDME, it is clear the protein VR lifetimes at a given  $\nu_{\text{CO}}$  are noticeably shorter. Solvent effects appear to be the most likely explanation for the systematically faster VR in proteins compared to PHDME. It does not seem likely that the systematic difference could be due to the minor differences between PHDME and PPIX.

In Mb, the solvent is a protein matrix with polar amino acid residues in the heme pocket (e.g., the distal histidine). In our PHDME experiments, the solvent was CH<sub>2</sub>Cl<sub>2</sub>. We know in principle that solvent effects are capable of increasing the VR enough to account for the Mb to PHDME differences seen in Figure 8, because these differences are comparable to the effects of changing CH<sub>2</sub>Cl<sub>2</sub> to DBP, as seen in Figure 5. It is well-known that electrostatic interactions between residues in the heme pocket and heme–CO can account for the different  $\nu_{\text{CO}}$  values in heme proteins.<sup>22,24–26</sup> The question arises whether the protein affects the VR rate simply by affecting the back-bonding and the through  $\pi$ -bond coupling between heme and CO or whether specific interactions between protein and CO permit CO-to-protein vibrational energy transfer. In our study

of mutant heme protein VR, we argued that CO to protein vibrational energy transfer was not likely to be significant.<sup>3</sup> If specific interactions between CO and the protein were responsible for carbonyl VR, then a rather complicated dependence of the VR rate on the details of the protein structure would be expected to result. Instead, a very simple linear lifetime–frequency correlation is observed.<sup>3,4</sup>

## VI. Summary and Conclusions

A large number of heme and porphyrin complexes were synthesized using different metal atoms M (M = Fe, Ru, Os) and different proximal ligands (imidazoles and pyridines). A remarkable correlation between carbonyl frequency  $\nu_{\text{CO}}$  and carbonyl vibrational relaxation (VR) lifetime in these complexes in CH<sub>2</sub>Cl<sub>2</sub> solvent was found, using mid-IR pump–probe experiments to directly measure the rate of energy loss from vibrationally excited CO. The vibrational lifetime decreases as  $\nu_{\text{CO}}$  decreases. The observed correlation is consistent with a linear relation between vibrational decay rate and  $\nu_{\text{CO}}$ . The fact that structural changes of the complexes strongly affect VR, whereas a series of different chlorinated hydrocarbon solvents do not, indicates the predominant VR process in CH<sub>2</sub>Cl<sub>2</sub> solvent is an intramolecular CO-to-porphyrin vibrational energy transfer rather than an intermolecular CO-to-solvent transfer. Isotope effect experiments show that the relationship between lifetime and frequency occurs because the frequency shift of  $\nu_{\text{CO}}$  is related to the strength of anharmonic coupling between CO and porphyrin. Experiments with different metal atoms (Fe, Ru, Os) show the most important anharmonic coupling involves the M–CO  $\pi$ -bonding. Vibrational energy relaxation of CO occurs mainly by through  $\pi$ -bond anharmonic coupling to heme or porphyrin.

The through  $\pi$ -bond anharmonic coupling model satisfactorily explains the most significant finding in this work, the lifetime–frequency correlation. Other, more subtle features of our data, however, require more study. First, there is a systematic difference in the lifetime–frequency correlation between a heme, PHDME, a porphyrin, TPP, and myoglobin (PPIX plus protein). At a given value of  $\nu_{\text{CO}}$ , the VR lifetime is shortest in Mb, longer in TPP, and longest in PHDME. Second, a proximal ligand which makes a metal–phosphorus bond does not obey the same lifetime–frequency correlation seen with imidazoles and pyridines which make a metal–nitrogen bond. We do not yet know whether these more subtle features involve interactions which affect the frequency without much affecting the lifetime, which affect the lifetime without much affecting the frequency or a combination of both.

One of the goals of our work is to develop a systematic understanding of the relationships between VR and molecular structure. Over many years of study, it was generally found that even relatively small structural changes in molecules may have large and presently unpredictable effects on VR. The CO–porphyrin systems we are studying are unique in this respect: by changing the structure in well-defined and well-controlled ways, we are able to essentially continuously tune the CO vibrational relaxation rate over a substantial range spanning about a factor of 4.

**Acknowledgment.** This research was supported by the Office of Naval Research, Biology Division, through Contract NOOO14-95-1-0259 (D.D.D. and J.R.H.). D.D.D. and J.R.H. acknowledge additional support from National Science Foundation Grant DMR-94-04806. K.S. and C.Z. acknowledge support from National Institutes of Health Grant PHS 5RO1-HL-25934. C.Z. thanks the National Science Foundation for fellowship

support. The work at Stanford University was supported by the Medical Free Electron Laser Program, through the Office of Naval Research, by Contract NOOO14-91-C-0170. M.D.F. acknowledges additional support from National Science Foundation Grant DMR-93-22504. We thank Michael M. Rosenblatt for synthesizing the COPRO complexes. We thank Prof. Alan Schwettman and Prof. Todd Smith and their research groups at the Stanford Free Electron Laser Center for making it possible to perform these experiments.

## References and Notes

- (1) Dlott, D. D.; Fayer, M. D.; Hill, J. R.; Rella, C. W.; Suslick, K. S.; Ziegler, C. J. *J. Am. Chem. Soc.* **1996**, *118*, 7853.
- (2) Hill, J. R.; Tokmakoff, A.; Peterson, K. A.; Sauter, B.; Zimdars, D.; Dlott, D. D.; Fayer, M. D. *J. Phys. Chem.* **1994**, *98*, 11213.
- (3) Hill, J. R.; Dlott, D. D.; Rella, C. A.; Peterson, K. A.; Decatur, S. M.; Boxer, S. G.; Fayer, M. D., *J. Phys. Chem.* **1996**, *100*, 12100.
- (4) Hill, J. R., Dlott, D. D.; Rella, C. W.; Smith, T. A.; Schwettman, H. A.; Peterson, K.; Kwok, A.; Rector, K.; Fayer, M. D. *Biospectroscopy* **1996**, *2*, 277.
- (5) Hochstrasser, R. M. *Proc. SPIE—Int. Soc. Opt. Eng.* **1992**, *1921*, 16.
- (6) Owrutsky, J. C.; Li, M.; Locke, B.; Hochstrasser, R. M. *J. Phys. Chem.* **1995**, *99*, 4842.
- (7) Kenkre, V. M.; Tokmakoff, A.; Fayer, M. D. *J. Chem. Phys.* **1994**, *101*, 10618.
- (8) Cotton, F. A.; Wilkinson, G. *Advanced Inorganic Chemistry*, 5th ed.; Wiley-Interscience: New York, 1988.
- (9) Seeley, G.; Keyes, T. *J. Chem. Phys.* **1989**, *91*, 5581. Xu, B.-C.; Stratt, R. M. *J. Chem. Phys.* **1990**, *92*, 1923. Wu, T. M.; Loring, R. F. *J. Chem. Phys.* **1992**, *97*, 8568.
- (10) Antonini, E.; Brunori, M. *Hemoglobin and Myoglobin in their Reactions with Ligands*; North-Holland: Amsterdam, 1971.
- (11) Hill, J. R.; Dlott, D. D.; Fayer, M. D.; Peterson, K. A.; Rella, C. W.; Rosenblatt, M. M.; Suslick, K. S.; Ziegler, C. J. *Chem. Phys. Lett.* **1995**, *244*, 218.
- (12) Barley, M.; Becker, J. Y.; Domazetis, G.; Dolphin D.; James, B. R. *Can. J. Chem.* **1987**, *61*, 2389.
- (13) Che, C. M.; Poon, C. K.; Chung W. C.; Gray, H. B. *Inorg. Chem.* **1985**, *24*, 1277.
- (14) Heilweil, E. J.; Cavanagh, R. R.; Stephenson, J. C. *Chem. Phys. Lett.* **1987**, *134*, 181. Heilweil, E. J.; Cavanagh, R. R.; Stephenson, J. C. *J. Chem. Phys.* **1988**, *89*, 230.
- (15) Tokmakoff, A.; Sauter, B.; Fayer, M. D. *J. Chem. Phys.* **1994**, *100*, 9035.
- (16) Tokmakoff, A.; Zimdars, D.; Sauter, B.; Francis, R. S.; Kwok, R. S.; Fayer, M. D. *J. Chem. Phys.* **1994**, *101*, 1741.
- (17) Tokmakoff, A.; Urdahl, R. S.; Zimdars, D.; Frances, R. S.; Kwok, A. S.; Fayer, M. D. *J. Chem. Phys.* **1995**, *102*, 3919.
- (18) Velsko, S.; Oxtoby, D. W. *J. Chem. Phys.* **1980**, *72*, 2260.
- (19) Levy, D. *Laser Spectroscopy of Cold Gas-Phase Molecules. In Annu. Rev. Phys. Chem.; Rabinovitch, B. S., Ed.; Annual Reviews, Inc.: Palo Alto, CA, 1980; Vol. 31; pp 197.*
- (20) Li, X. Y.; Spiro, T. G. *J. Am. Chem. Soc.* **1988**, *110*, 6024.
- (21) Park, K. D.; Guo, K.; Adebodun, F.; Chiu, M. L.; Sligar, S. G.; Oldfield, E. *Biochemistry* **1991**, *30*, 2333.
- (22) Oldfield, E.; Guo, K.; Augspurger J. D.; Dykstra, C. E. *J. Am. Chem. Soc.* **1991**, *113*, 7537.
- (23) Braterman, P. S. *Metal Carbonyl Spectra*, Academic Press: London, 1975.
- (24) Ray, G. B.; Li, X.-Y.; Ibers, J. A.; Sessler, J. L.; Spiro, T. G. *J. Am. Chem. Soc.* **1994**, *116*, 162.
- (25) Balasubramanian, S.; Lambright, D. G.; Boxer, S. G. *Proc. Natl. Acad. Sci. U.S.A.* **1993**, *90*, 4718. Decatur, S. M.; Boxer, S. G. *Biochem. Biophys. Res. Commun.* **1995**, *212*, 159.
- (26) Springer, B. A.; Sligar, S. G.; Olson, J. S.; Phillips, G. N., Jr. *Chem. Rev.* **1994**, *94*, 699.
- (27) Herzberg, G. *Molecular Spectra and Molecular Structure, II. Infrared and Raman Spectra*; Van Nostrand Reinhold: New York, 1945; pp 173–4.
- (28) Schick, G. A.; Bocian, D. F. *J. Am. Chem. Soc.* **1984**, *106*, 1682.
- (29) Kim, D.; Su, Y. O.; Spiro, T. G. *Inorg. Chem.* **1986**, *25*, 3993.
- (30) Benjamin, I.; Reinhardt, W. P. *J. Chem. Phys.* **1989**, *90*, 7535.
- (31) Meier, W.; Schrader, B. *Raman/IR Atlas of Organic Compounds*; Verlag Chemie: Dortmund, 1974.
- (32) Moore, P.; Tokmakoff, A.; Keyes, T.; Fayer, M. D. *J. Chem. Phys.* **1995**, *103*, 3325.

JP961418F